RESEARCH PAPER

Development, Characterization, and In-Vivo Toxicological Assessment of Hyaluronic Acid-Coated Liposomes for Enhanced Intranasal Brain Delivery of Rivastigmine Tartrate

Mansha Singhai[1]*, Aman Kansare[2]

[1] *Research Scholar, Faculty of Pharmacy, Oriental University, Indore, Madhya Pradesh, 453555, India.*
[2] *Associate Professor, Faculty of Pharmacy, Oriental University, Indore, Madhya Pradesh, 453555, India.*
Corresponding Author
Mansha Singhai
Email: jainmansha1@gmail.com

ABSTRACT

This study reports the development and evaluation of a hyaluronic acid–coated liposomal formulation (HALPs) for the intranasal delivery rivastigmine tartrate to the brain. The optimized formulation exhibited a high drug entrapment efficiency of 65.78 ± 6.6% and a nanosize vesicle diameter of 121.36±3.05 nm. The robustness of the formulation variables was confirmed by statistical validation and systematic optimization using a Box-Behnken design (BBD). Comprehensive physicochemical and ultrastructural characterization, including Fourier transform infrared spectroscopy (FT-IR) and transmission electron microscopy (TEM), verified formulation compatibility, uniform vesicle morphology, and structural integrity. Stability studies demonstrated that the optimized formulation retained its physicochemical properties over a three-month period under both refrigerated (4 °C) and ambient (25 °C) storage conditions. Furthermore, the optimized formulation (HALPs-F18) exhibited a sustained drug release profile extending up to six hours. In-vivo acute intranasal toxicity studies in Wistar rats revealed no signs of systemic toxicity or nasal mucosal irritation, confirming the safety and biocompatibility of the developed liposomal system. Overall, these findings suggest that hyaluronic acid-coated liposomes (HALPs-F18) constitute a stable, safe, and efficient intranasal drug delivery platform with enhanced potential for targeted central nervous system delivery, highlighting their promise as a therapeutic strategy for brain-targeted drug administration...

Keywords: *Intranasal delivery, Hyaluronic acid, Liposome, Alzheimer's disease..*

How to cite this article: Singhai M, Kansare A.., Development, Characterization, and In-Vivo Toxicological Assessment of Hyaluronic Acid-Coated Liposomes for Enhanced Intranasal Brain Delivery of Rivastigmine Tartrate . Int J Drug Deliv Technol. 2026;16(79s):1217-1235. DOI: 10.25258/ijddt.16.79s.200..

Source of support: Nil.

Conflict of interest: None

Highlights

- Hyaluronic acid-coated liposomes were successfully developed using the thin-film hydration technique.
- The optimized HA-coated liposomes exhibited a desirable particle size distribution and stable zeta potential.
- HA coating enhanced the physicochemical stability of liposomes during refrigerated storage.
- In-vivo studies demonstrated that the HA-coated liposomal formulation was safe, biocompatible, and non-toxic following intranasal administration

1. INTRODUCTION

Alzheimer's disease (AD) is a progressive neurological disorder that gradually impairs memory, thinking, attention, and decision making, making it difficult for individuals to carry out daily activities. As the most common type of dementia, it involves a steady decline in at least two cognitive areas- such as memory, language, behaviour, personality, executive function, and visuospatial skills- and accounts for approximately 80% of all dementia cases [1]. The World Alzheimer Report (2022) estimated that around 55 million people globally are living with AD or other related dementia, with projections indicating this number could increase to 82 million by 2030 and 138 million by 2050 [2]. This

**Author for Correspondence: jainmansha1@gmail.com*

escalating prevalence underscores the profound global public health burden posed by AD.

The United States has approved rivastigmine tartrate, memantine, donepezil, and galantamine for the management of AD symptoms by the Food and Drug Administration [3]. Numerous studies have demonstrated the neuroprotective potential of different medication systems based on nano-formulations in addition to these medicinal medicines. Their antioxidant, anti-inflammatory, and anti-apoptotic mechanisms have shown promising outcomes in both preclinical and clinical studies, positioning nanocarrier-mediated therapeutics as emerging candidates for improved AD treatment [4]. A number of theories have been put out to explain the fundamental mechanisms of AD pathogenesis, such as the accumulation of extracellular amyloid-β plaques, oxidative stress, apolipoprotein E, hyperphosphorylated tau, and cholinergic deficiency.

Rivastigmine tartrate, a cholinesterase inhibitor, remains one of the most widely used medications for the symptomatic relief of AD. However, conventional formulations such as oral tablets and transdermal patches often fail to achieve optimal therapeutic efficacy due to limited brain bioavailability and dose-dependent adverse effects [5]. Consequently, interest has grown in nose-to-brain delivery approaches, which offer a non-invasive and patient-friendly alternative. The intranasal route allows therapeutic medicines to be directly transported to the central nervous system when combined with a suitable formulation approach, significantly increasing the effectiveness of brain-targeting [6].

Several studies have demonstrated the potential of intranasal systems for rivastigmine tartrate delivery. Shah B.M. et al. (2015) reported increased brain concentrations following intranasal administration of a rivastigmine tartrate microemulsion [7]. Nageeb El-Helaly S. et al. (2017) observed improved therapeutic efficacy using liposomal dispersions of intranasally administered rivastigmine tartrate [8]. More recently, Guo H. *et al.* 2024, successfully formulated a rivastigmine tartrate nasal spray that enhanced olfactory deposition and improved brain delivery [9]. In addition, Lee D. *et al.* 2024, demonstrated significantly enhanced brain distribution using liposomes co-loaded with donepezil, memantine, and BACE-1 siRNA through the intranasal route. All of these trials together offer strong evidence that nose-to-brain administration is a successful strategy for increasing rivastigmine tartrate availability in the brain [10].

Building on this basis, the current study sought to create mucoadhesive liposomes coated with hyaluronic acid (HA) that encapsulated rivastigmine tartrate in order to promote nose-to-brain (N2B) transit and, eventually, therapeutic efficacy. Because liposomes (LPs) are suitable for intranasal N2B delivery and can shield the drug from enzymatic degradation, they were chosen as the drug delivery system [6]. HA was incorporated as a functional excipient because of its strong mucoadhesive properties, ability to prolong nasal residence time, and potential to facilitate receptor-mediated absorption [11]. Using this formulation strategy, HA-coated liposomes were developed and optimized in the first phase of the study and subsequently subjected to comprehensive physicochemical characterization.

HA, a naturally occurring and biocompatible polymer has been shown to enhance mucosal drug absorption due to its excellent mucoadhesive properties [12]. Several studies have reported that HA-based formulations improve nasal residence time, drug permeation, and brain-targeting efficiency, resulting in enhanced therapeutic outcomes. Supporting this, Serri C. *et al.,* 2025, developed HA-functionalized lipid–polymer nanoparticles (LPNs) for intranasal delivery of dimethyl fumarate (DMF), demonstrating improved nanoparticle stability, enhanced mucoadhesion, prolonged nasal residence, and receptor-mediated uptake. Evaluations conducted both *in vitro* and *in vivo* verified the effective nose-to-brain transport, low cytotoxicity, and quick cellular absorption [13]. Similarly, AbouElhassan K.M. *et al.,* 2022 formulated HA-decorated nano-transbilosomes for intranasal citicoline delivery, achieving high drug entrapment, sustained release, enhanced brain targeting, and neuroprotection in an Alzheimer's rat model [14].

Combined, these results support the development of HA-functionalized rivastigmine tartrate -loaded liposome formulation (HALPs) in the present study, highlighting the critical role of HA in enhancing therapeutic efficacy and bolstering its use in nasal formulations for drug delivery to specific brain regions.

The formulation development process was guided by an organized Quality by Design (QbD) framework. The critical material attributes (CMAs) and critical process parameters (CPPs) that may affect the primary quality characteristics of liposomes loaded with rivastigmine tartrate were determined by means of a methodical risk assessment. These insights were used to optimize the formulation using statistically based experimental design

tools, ensuring that all targeted quality parameters were achieved within the desired acceptance limits. The optimized liposomal system was subsequently subjected to comprehensive *in vitro* and *in vivo* evaluations to assess its physicochemical properties, stability, performance, and therapeutic potential. This study aimed to develop and characterize hyaluronic acid (HA)-grafted mucoadhesive liposomal formulation. The formulation was optimized using a Box–Behnken design (BBD). The optimized HALPs were characterized for particle size, morphology, entrapment efficiency, zeta potential, polydispersity index (PDI), and solid-state properties. The developed formulations were evaluated by drug release, stability, and behavioral studies in rats. The findings demonstrated the potential of the optimized HALPs as an effective and promising intranasal drug delivery system for targeted brain therapy.

In order to treat Alzheimer's, the formulation seeks to increase brain bioavailability and decrease mucociliary clearance.

2. Material and methods

2.1. Chemicals

A Rivastigmine tartrate gift sample (CAS No. 129101-54-8) was acquired from Alembic Pharmaceuticals Limited in Vadodara, India. Gift samples of soybean lecithin, Lipoid S100® (LS100) (CAS No. 8002-43-5), and N-(carbonyl-methoxypolyethylene glycol-2000)-1, 2-distearoyl-sn-glycero-3-phosphoethanolamine, sodium salt (mDSPE-PEG2000) (CAS No. 147867-65-0) were sent by Lipoid® GmbH (Ludwigshafen, Germany). Medium-molecular-weight hyaluronic acid (HA) (CAS No. 9004-61-9), N-hydroxysuccinimide (NHS) (CAS No. 6066-82-6), 1-ethyl-3-(3-dimethylaminopropyl) carbodiimide (EDC) (CAS No. 25952-53-8), cholesterol (CHOL) (CAS No. 57-88-5), dimethyl sulfoxide (DMSO) (CAS No. 67-68-5), and disodium hydrogen phosphate (CAS No. 7558-79-4) were all provided by Sigma-Aldrich (Powai, Mumbai, India). Every additional chemical and reagent utilized in the investigation was of HPLC quality.

2.2. Animals and Ethical Approval

Adult Wistar albino rats, weighing 120–170 g and aged 8–10 weeks, were obtained from the Animal house facility of Adina Institute of Pharmaceutical Sciences Sagar, Madhya Pradesh. The experimental design was authorized by the Institutional Animal Ethics Committee (IAEC) of Adina Institute of Pharmaceutical Sciences, Sagar, Madhya Pradesh, India [Committee for Control and Supervision of Experiments on Animals (CCSEA registration number: 1546/PO/Re/S/11/CCSEA: 19/2/2026)]. The rules for reporting animal experiments, Animal Research: Reporting of *in vivo* Experiments (ARRIVE) 2.0, were followed in all animal-based investigations. In polypropylene cages with a 12:12 h light-dark cycle, the animals were kept in conditions with regulated humidity and temperature (25°C ± 2°C; 55–65%).

2.3. Preparation of liposomes

Liposomes were prepared using the thin-film hydration method with Lipoid S100, cholesterol, and DSPE-PEG2000 as the lipid components. The lipids were dissolved in a methanol–chloroform mixture in a 250 mL round-bottom flask. The organic solvents were then removed under reduced pressure using a rotary evaporator maintained at 40 °C and 60 rpm, resulting in the formation of a thin, uniform lipid film on the inner surface of the flask. The dried lipid film was hydrated with phosphate-buffered saline (PBS, pH 7.4) containing rivastigmine tartrate to facilitate drug encapsulation. The resulting dispersion was allowed to stand overnight to ensure complete hydration of the lipid film and the formation of multilamellar vesicles (MLVs) (**Figure 1**). Thereafter, the liposomal dispersion was sonicated in an ice bath for 6 minutes using alternating 20-second ON/OFF cycles to reduce the vesicle size while maintaining a constant temperature [15, 16].

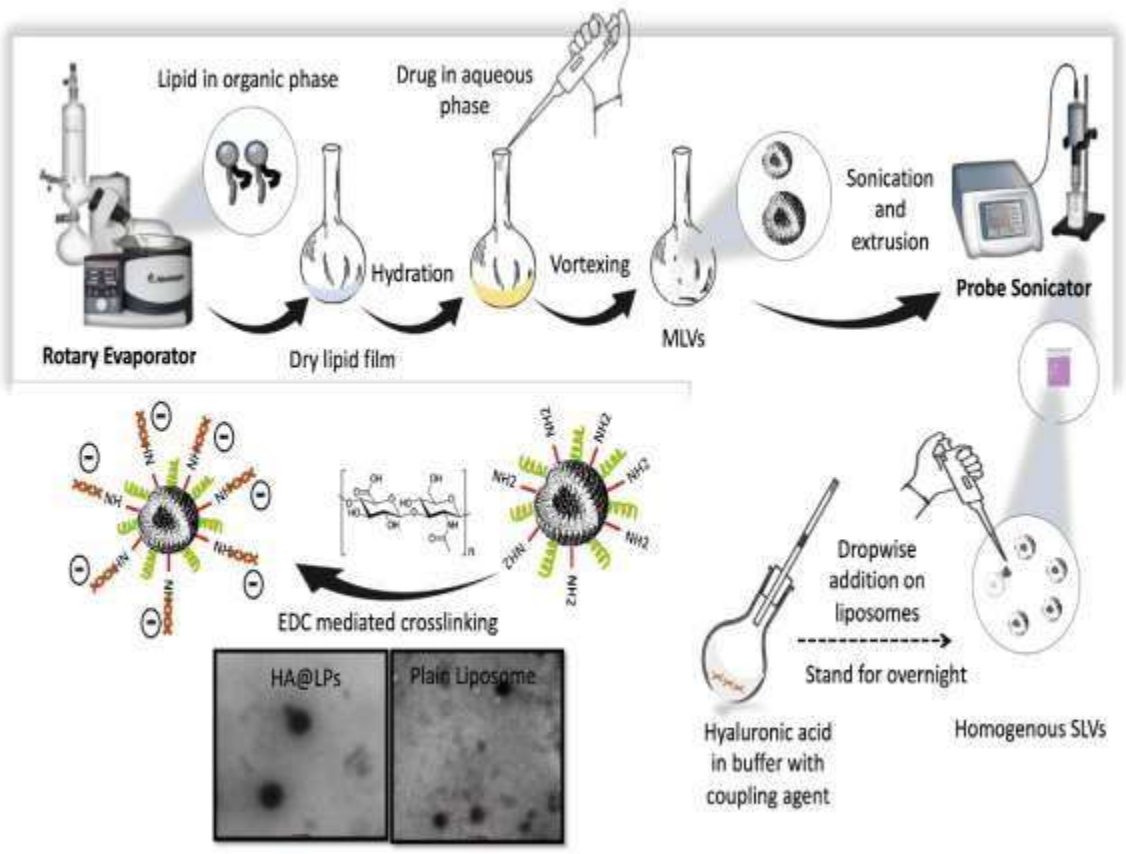

Figure 1: Stepwise schematic illustration of the formulation process of HALPs liposomes

2.4. Preparation of hyaluronic acid conjugated liposomes (HALPs)

Stock solutions of hyaluronic acid (HA), N-hydroxysuccinimide (NHS), and 1-ethyl-3-(3-dimethylaminopropyl) carbodiimide (EDC) were prepared in deionized water at a concentration of 1 mg/mL. HA (0.3 mg) was activated by adding NHS (0.1 mg) and EDC (0.3 mg), and the reaction mixture was incubated overnight at room temperature (25 °C) as showed in **Figure 1**. Activated HA (0.1 mL) was then added dropwise to 0.9 mL of the liposomal dispersion under continuous magnetic stirring to obtain HA-coated liposomes (HALPs). The dispersion was stirred for 1 h and further incubated overnight at room temperature to ensure complete HA conjugation. The resulting HALPs were lyophilized and characterized by Fourier transform infrared (FT-IR) spectroscopy to confirm successful HA coating through amide bond formation [17].

2.5. Experimental design and optimization

The liposomal formulation was optimized using Design-Expert® software (version 13.0.5.0, Stat-Ease Inc., Minneapolis, MN, USA) based on a three-factor, three-level Box–Behnken design (BBD) with three variables and three levels (−1, 0, +1), including centre points. Three independent variables were evaluated: lipid ratio (Lipoid S100; A), hyaluronic acid (HA) concentration (B), and sonication time (C). The variables were investigated at three levels: lipid ratio (6:3, 7:3, and 8:3), HA concentration (0.05, 0.10, and 0.15 mg/mL), and sonication time (2, 5, and 8 min). A total of 17 experimental runs, including centre points, were generated. Vesicle size (Y_1) and entrapment efficiency (Y_2) were selected as the dependent response variables for optimization.

2.6. Characterization of formulations

2.6.1. Vesicle size and zeta potential

The vesicle size and zeta potential of HALPs were determined by dynamic light scattering (DLS) using a NanoPlus Zeta/Nanoparticle Analyzer (Norcross, GA, USA). Samples (100 µL) were diluted to 1 mL with deionized water and analyzed in triplicate using disposable cuvettes [18].

*Author for Correspondence: jainmansha1@gmail.com

2.6.2. Determination of percentage entrapment efficiency (%EE)

The entrapment efficiency (%EE) of HALPs was determined using the liposome disruption method. For total drug estimation, 10 µL of the formulation was disrupted with 100 µL of acetonitrile under vortex mixing, followed by the addition of 100 µL of 50% aqueous methanol. The mixture was centrifuged at 60,000 rpm for 10 min, and the supernatant was analyzed by HPLC (n = 3). To determine the free (unencapsulated) drug, 100 µL of the liposomal dispersion was centrifuged at 60,000 rpm for 10 min. An aliquot (50 µL) of the supernatant was diluted to 2 mL with the appropriate diluent and analyzed by HPLC (n = 3) [17,19]. The %EE was calculated from the difference between the total and free drug concentrations using HPLC calibration curves and expressed by the following equation:

$$\%EE = \frac{\text{Total drug} - \text{Free drug}}{\text{Total drug}} \times 100 \qquad (1)$$

2.6.3. Structural Analysis Using TEM

The surface morphology of HALPs was examined using transmission electron microscopy (TEM) (Thermo Scientific™ Talos L120C, Jamia Hamdard). Prior to imaging, the samples were negatively stained with 1% (w/v) phosphotungstic acid and observed at an accelerating voltage of 100 kV.

2.6.4. FT-IR Spectroscopic Analysis

FT-IR spectroscopy was performed to confirm the conjugation of HA to DSPE-PEG2000-functionalized liposomes via EDC/NHS-mediated carbodiimide coupling. Lyophilized samples of HALPs, HA, and DSPE-PEG2000 were individually mixed with dry potassium bromide (KBr) powder and finely ground using a mortar and pestle. The mixture was compressed into a transparent pellet using a die set and hand press, and the pellet was analyzed by Fourier transform infrared (FT-IR) spectroscopy (Alpha-T, Model 200791). Spectra of HALPs, DSPE-PEG2000, and HA were recorded and compared [17,20,21].

2.6.5. HPLC analysis

Rivastigmine tartrate was quantified using a high-performance liquid chromatography (HPLC) system (Shimadzu Prominence-i LC-20AT 3D Plus) equipped with an LC-20AT pump and an SPD-20A UV/Vis detector. Chromatographic conditions were optimized based on previously reported methods with minor modifications [22,23]. Separation was achieved on a reversed-phase C18 column (Luna 5 µm, 250 × 4.6 mm, Phenomenex) maintained at 40 °C, using a mobile phase consisting of acetonitrile and phosphate-buffered saline (PBS, pH 3.0) (40:60, v/v) at a flow rate of 1.0 mL/min. A 20 µL aliquot of each standard and sample solution was injected in duplicate, and detection was carried out at 203 nm.

The calibration curve, constructed by plotting peak area against rivastigmine tartrate concentration, exhibited good linearity with the regression equation y = 390.12x + 587.71, where y represents the peak area and x the rivastigmine tartrate concentration.

2.7. *In-vitro* drug release studies

The *in-vitro* drug release study was conducted using a dialysis sac method maintained at 37 ± 0.5 °C. The receptor compartment was filled with 20 mL of phosphate buffer (pH 6.4) and continuously stirred at 100 rpm to ensure uniform mixing and maintain sink conditions [7]. A dialysis membrane (molecular weight cut-off 12 kDa; HiMedia, India), previously hydrated in distilled water, was placed between the donor and receptor compartments to act as the diffusion barrier. At predetermined time intervals, aliquots were withdrawn from the receptor compartment and immediately replaced with an equal volume of fresh phosphate buffer to maintain a constant volume and sink conditions throughout the experiment. The collected samples were analyzed using HPLC to determine the amount of drug released [24].

2.8. Stability study

A stability study was performed to assess drug leakage and the physicochemical stability of the optimized coated liposomal formulation during storage. The formulation was stored in hermetically sealed 5 mL clear glass vials under two different conditions: room temperature (25 ± 2 °C) and refrigerated temperature (4 ± 2 °C) for a period of three months. At predetermined time intervals, samples were withdrawn and evaluated for particle size and entrapment efficiency to determine any changes in vesicle characteristics, drug retention, and overall formulation stability throughout the storage period [25,26].

2.9. *In-vivo* studies

2.9.1. Dose Selection

Based on previous intranasal studies demonstrating no adverse effects at this dose, acute toxicity was evaluated using a limit dose of 0.5 mg/kg [27]. To ensure nasal tolerability, the liposomal formulation was diluted with

phosphate-buffered saline (PBS) and administered at a volume of 50 µL per nostril (total 100 µL per rat). The vehicle control consisted of PBS alone, while the plain liposome control comprised drug-free liposomes prepared using the same formulation procedure as the test formulation.

2.9.2. Intranasal Administration Procedure

For intranasal administration, each animal was gently restrained in an upright position and formulation was administered using a micropipette, with the tip positioned at the entrance of the nostril. A volume of 50 µL was delivered alternately into each nostril of rat. The formulation was dispensed in synchrony with the animal's inspiration to facilitate capillary absorption and enhance deposition within the nasal cavity [28].

2.9.3. Experimental Design

Eighteen animals were randomly divided into three experimental groups (9 males and 9 females): (1) plain liposomes, (2) rivastigmine tartrate -loaded liposomes (100 µg/rat), and (3) vehicle control (PBS). After dosing, all animals were observed for 14 days to evaluate any changes in their body or behaviors, body posture, breathing, sedation, drowsiness, mortality, diarrhoea, skin color, fur conditions, coma, and eye color. Particular attention was given to the first 30 minutes after dosing, during which the animals were closely monitored for immediate clinical signs. On Day 14, the number of surviving animals was recorded, and all survivors were go for autopsy. Major organs, including the lungs, liver, kidneys, spleen, heart, intestines, and uterus, were carefully examined macroscopically for any visible abnormalities or pathological changes.

In order to continue with the examination of the biochemical and haematological markers, blood was also drawn.

2.10.4. Sample collection

The animals were fasted overnight and anesthetized prior to blood collection. Blood samples were collected by cardiac puncture. One portion of the blood was collected into EDTA-coated BD Vacutainer® tubes for hematological analysis. The remaining blood was transferred to red-top BD Vacutainer® tubes and allowed to clot at room temperature for 25–30 minutes. The clotted samples were then centrifuged at 1,500 × g for 15 minutes at 4 °C to separate the serum. The resulting serum supernatant was collected and used for further biochemical analyses.

2.10.5. Haematology analysis

These parameters were assessed using a haematological auto-analyzer: hemoglobin (Hb) concentration, platelet count, red blood cell (RBC) count, packed cell volume (PCV), mean corpuscular volume (MCV), mean corpuscular hemoglobin (MCH), total leukocyte count (TLC), and differential leucocytic count (neutrophil, lymphocyte, eosinophil, monocyte, and basophil).

2.10.6. Biochemical analysis

The following parameters were evaluated: (a) lipid profile assay, which included tests for total cholesterol, triglycerides, high density lipid, and very low density lipids; (b) liver markers, which included the enzymes aspartate aminotransferase (AST), alanine aminotransferase (ALT), alkaline phosphatase (ALP), total bilirubin, and direct bilirubin; (c) kidney function test panel, which included blood urea nitrogen, uric acid, and creatinine; (d) protein estimation, which included total protein and albumin; (e) calcium estimation; and (f) glucose analysis. In accordance with the manufacturer's instructions for the kits provided by Erba Diagnostics, serum samples were examined using the semi-automated clinical chemistry analyzer Erba Chem 5X.

2.11. Statistical analysis

All experimental data were expressed as mean ± standard deviation (SD). Statistical analyses were performed using GraphPad Prism software (version 8.0; GraphPad Software, San Diego, CA, USA). Differences among multiple groups were evaluated by one-way analysis of variance (ANOVA) followed by Tukey's post hoc multiple comparison test. A value of $p < 0.05$ was considered statistically significant.

3. Results

3.1. Optimization of HALPs Using Design of Experiments (DoE)

The HALPs were prepared using the thin-film hydration method and optimized through a Box–Behnken Design (BBD). The experimental design was generated using Design-Expert® software, which evaluated the influence of the selected independent variables on the critical quality attributes, such as vesicle size and entrapment efficiency. After characterization of all experimental batches, the obtained data were fitted to appropriate statistical models, and analysis of variance (ANOVA) was performed to determine the significance of the formulation variables. Response surface and contour plots were generated to visualize the individual and interactive effects of the variables on the selected responses (**Table 1 and Fig. 2**).

Table 1: Design of Experiments (DoE): Factors and responses of HALPs formulations

Factor code	**Factor name**		**Factor level**			**Response Code**	
		-1		0	+1		
A	(Lipid: Cholesterol) Ratio	6:3		7:3	8:3	Y_1	Vesicle size (nm)
B	Concentration of HA (mg/ml)	0.05		0.1	0.15	Y_2	Entrapment efficiency (%)
C	Sonication time (min)	2		5	8		

Run	**Formulation Code**	**(Lipid: Cholesterol) Ratio**	**Concentration of HA (mg/ml)**	**Sonication Time (min)**	**Vesicle size (nm)**	**Entrapment efficiency (%)**
1	HALPs-F1	6	0.1	8	111.6±1.2	58.33±1.2
2	HALPs-F2	6	0.15	5	137.4±2.3	65.50±2.1
3	HALPs-F3	6	0.05	5	122.9±3.4	55.71±2.3
4	HALPs-F4	6	0.1	2	147.0±3.4	74.40±3.4
5	HALPs-F5	7	0.05	8	117.7±3.3	67.90±2.4
6	HALPs-F6	7	0.1	5	134.4±2.3	63.70±3.4
7	HALPs-F7	7	0.05	2	145.1±4.6	71.50±3.2
8	HALPs-F8	7	0.15	8	133.7±6.7	63.55±3.5
9	HALPs-F9	7	0.15	2	167.1±6.5	75.78±5.4
10	HALPs-F10	7	0.1	5	136.0±4.3	65.60±4.6
11	HALPs-F11	7	0.1	5	135.3±2.2	64.50±6.6
12	HALPs-F12	7	0.1	5	134.8±1.1	65.00±5.5
13	HALPs-F13	7	0.1	5	135.1±2.3	65.09±4.5
14	HALPs-F14	8	0.05	5	142.4±2.4	66.70±4.5
15	HALPs-F15	8	0.1	2	165.3±2.5	77.07±4.6
16	HALPs-F16	8	0.15	5	167.4±3.4	68.01±4.3
17	HALPs-F17	8	0.1	8	140.6±3.3	63.08±2.3

All formulations contain 10 mg RT.

* SD (Standard deviation of n = 3).

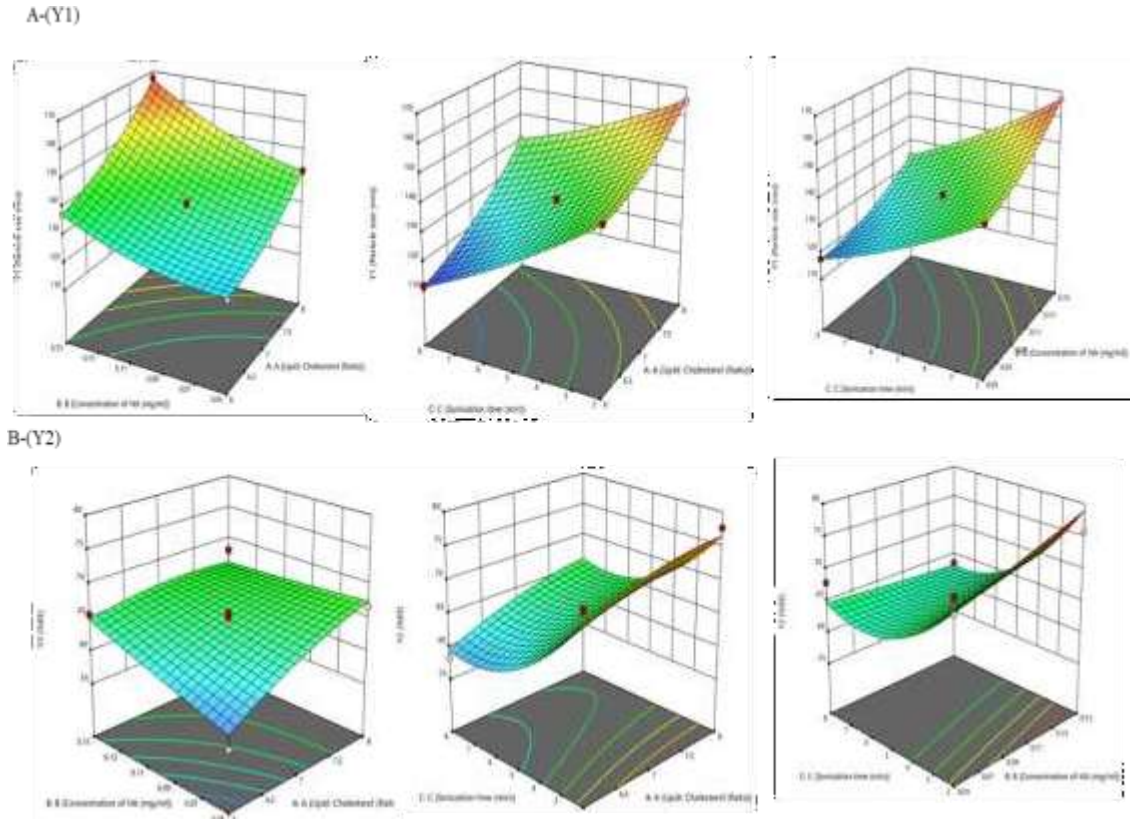

Figure 2: 3-D response plots showing how independent factors affect dependent variables (Y1 and Y2) are represented by A and B, where (A) is the particle size (nm) and (B) is the percentage of entrapment efficiency of HALPs-F1-F17 (n = 3)

The optimized formulation was selected based on the numerical optimization function provided by the software. Among the 28 predicted solutions, the first solution was chosen as the optimized formulation owing to its desirable balance between minimal vesicle size and maximum entrapment efficiency [29,30]. The optimized formulation exhibited an overall desirability value of 0.632, indicating acceptable agreement between the target and predicted responses. ANOVA confirmed that the selected formulation variables significantly influenced both vesicle size and %EE, while the response surface plots clearly demonstrated the interactions among the formulation factors.

The optimized HALPs showed a small vesicle size and high drug entrapment efficiency, indicating successful HA coating and their potential suitability for intranasal nose-to-brain drug delivery. Furthermore, the experimentally observed values showed relative prediction error of less than 0.5%, confirming the validity and robustness of the optimization model (**Table 2** and **Figure. 2).**

Table 2: (A) Regression model summary for the selected responses. (B) Optimized factor levels with predicted and experimental response values obtained through DoE

(A)					
Response	**Model**	**Adequate precision**	**R^2**	**Adjusted R^2**	**Predicted R^2**
Y1 (Particle size)	Linear and Quadratic	125.25	0.9994	0.9986	0.9956
Y2 (%EE)	Quadratic	10.7036	0.9096	0.7935	0.3596
(B)					
Factor				**Optimized level**	

X1: lipid: Cholesterol (Ratio)				7.51	
X2: Concentration of HA				0.50	
X3: Sonication time				8	
Response				Expected	Observed
Y1 (Particle size)				124.892	123.43
Y2 (%EE)				67.25±6.6	66.78

3.2. Physiological characterization of HALPs

3.2.1. Mean vesicle size

The physical stability and nose-to-brain transport efficiency of the formulation are directly impacted by mean vesicle size, making it a crucial quality measure. The vesicle diameters of HALPs-F1 to HALPs-F17 ranged from 111.6 ± 1.2 to 167.4 ± 3.4 nm, as showed in **Table 1**. The effect of formulation variables on vesicle size was described using quadratic polynomial model, as presented in **Figure 2**.

The Particle size (Y_1) was expressed by the following equation:

$$Y_1 = 135.12 + 12.10A + 9.69B - 15.11C + 2.63AB + 2.67AC - 1.50BC + 3.82A^2 + 3.59B^2 + 2.19C^2$$

Where **A, B and C** are independent variables. Positive coefficients for A and B increase vesicle size, while the negative coefficient of *C* reduces it. Interaction and quadratic terms highlight nonlinear and combined effects. The model demonstrated excellent fit ($R^2 = 0.9994$), and all terms were statistically significant. The optimized formulation (HALPs-F18) exhibited a vesicle size of 121.36 ± 3.05 nm, indicating an appropriate size for intranasal delivery (**Figure 3**)

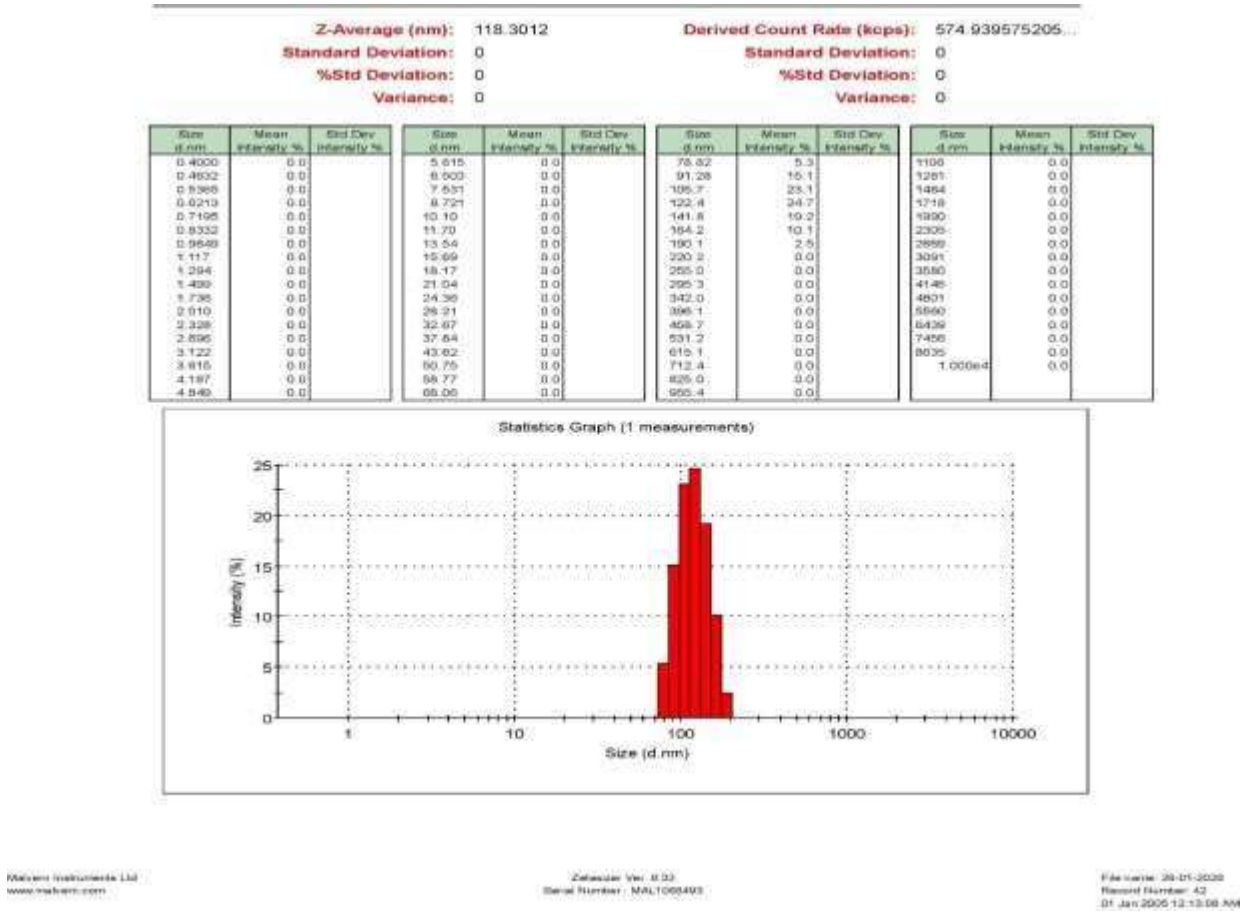

Figure 3: The vesicle size of optimized formulation HALPs-F18

3.2.2. Zeta Potential

The optimized HALPs-F18 formulation exhibited a zeta potential of −36.3 mV, indicating successful surface modification with hyaluronic acid. The pronounced negative surface charge is attributed to the ionization of the carboxyl groups present in the hyaluronic acid coating, confirming its effective adsorption onto the liposomal surface. A zeta potential value greater than -30 mV is generally considered indicative of good electrostatic stability, as it promotes strong repulsive forces between vesicles, thereby minimizing aggregation and enhancing colloidal stability. The high negative surface charge of the optimized formulation is expected to improve its physical stability during storage while maintaining uniform dispersion. Furthermore, this enhanced stability is advantageous for intranasal administration, as it helps preserve vesicle integrity, facilitates consistent nasal dispersion, and supports efficient nose-to-brain drug delivery.

3.2.3. Percentage Entrapment efficiency (%EE)

Entrapment efficiency is a crucial parameter for evaluating the system's stability and drug-loading capacity of liposomes. The range of % EE for formulations HALPs-F1 to HALPs-F17 was ranged from 55.71 ± 2.3% to 77.07 ± 4.6% demonstrating the influence of formulation variables on drug encapsulation (**Table 1 and Figure 2**). The relationship between the formulation variables and %EE was adequately described by a quadratic polynomial model indicating the presence of both individual and interaction effects among the variables. The developed model showed a good fit to the experimental data and was subsequently used to predict the optimal formulation conditions for maximizing drug entrapment efficiency.

The entrapment efficiency response (Y_2) was represented by the following equation:

$$Y_2 = 64.94 + 2.80A + 1.39B - 5.73C - 2.10AB + 0.54AC - 2.16BC - 1.03A^2 + 0.094B^2 + 4.65C^2$$

The quadratic polynomial equation demonstrated the influence of the independent formulation variables A, B, and C on the entrapment efficiency (%EE). The positive coefficients of variables A and B indicated a favorable effect on drug entrapment, suggesting that increasing these factors enhanced the %EE. In contrast, the negative coefficient of variable C indicated an inverse relationship, where increasing its level resulted in a reduction in entrapment efficiency. The presence of quadratic terms (A^2, B^2, and C^2) and interaction terms (AB, AC, and BC) further revealed the nonlinear behavior and combined effects of the formulation variables on %EE. The developed model exhibited a satisfactory fit with a coefficient of determination (R^2 = 0.9096), indicating strong agreement between the predicted and experimental values. The optimized formulation (HALPs-F18) achieved an entrapment efficiency of 65.78 ± 6.6%, validating the predictive capability of the optimization model and confirming the suitability of the selected formulation variables for the development of an efficient hyaluronic acid-coated liposomal drug delivery system.

3.3. Confirmation of hyaluronic acid conjugation

3.3.1. FT-IR analysis of HALPs

To verify the successful coating of HA on the liposomal surface and to evaluate the chemical compatibility between rivastigmine tartrate and the formulation excipients, FTIR spectroscopy was performed. **Figure 4** presents the FTIR spectra of (A): Rivastigmine Tartrate; (B): $DSPEPEG_{2000}$; (C): Hyaluronic acid; and (D): HALPs-F18

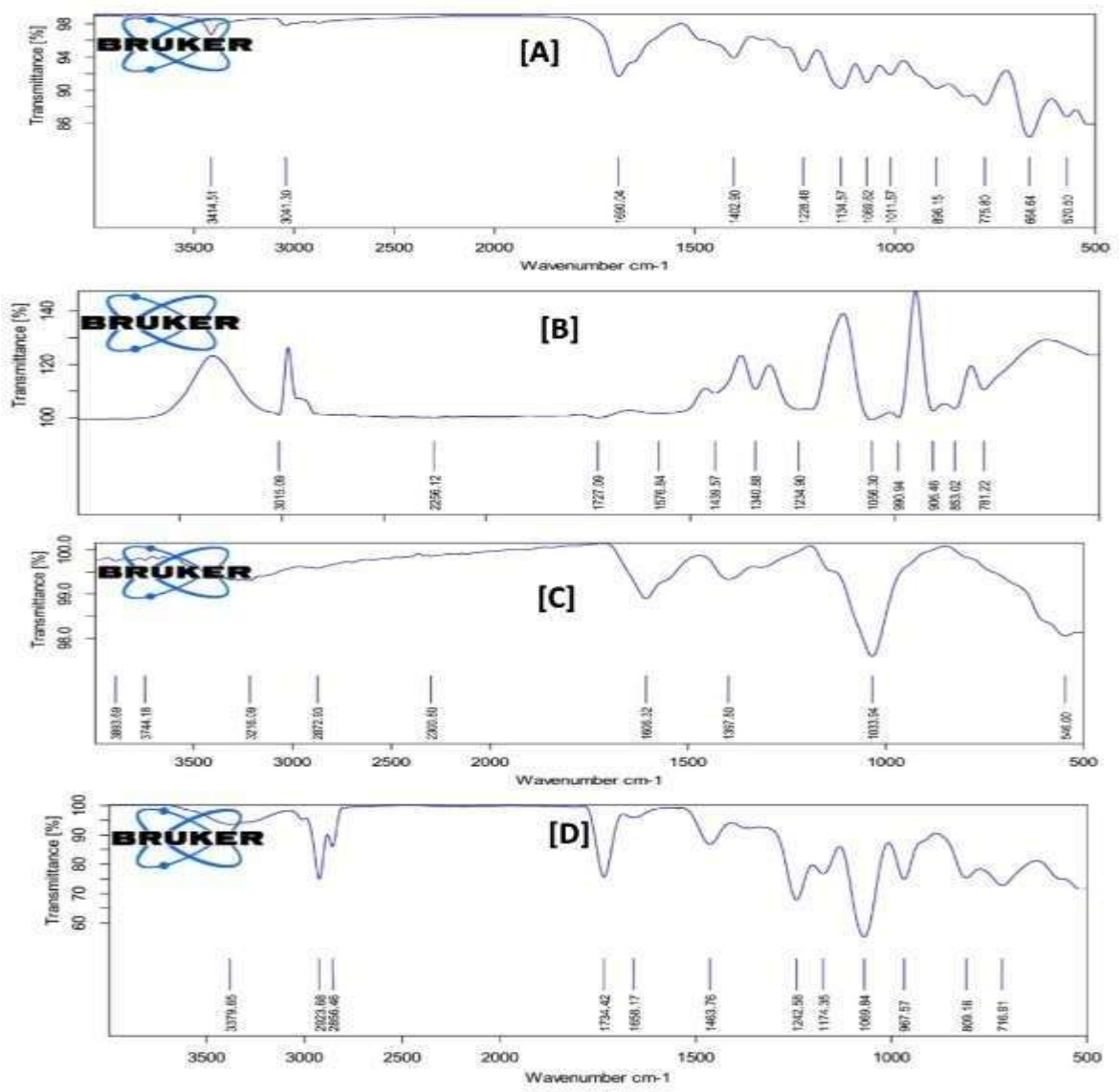

Figure 4: FTIR Spectra illustrating the characteristic functional groups of (A) Rivastigmine Tartrate; (B) DSPEPEG$_{2000}$; (C) Hyaluronic acid; and (D) HALPs-F18 formulation

The conjugation of Rivastigmine tartrate, DSPE-PEG2000, Hyaluronic acid, and HA-LPs-F18 are presented in **Figure 5**. FTIR spectroscopy was employed to confirm successful HA coating of the liposomal formulation and to evaluate the compatibility between rivastigmine tartrate and the formulation excipients. Rivastigmine tartrate exhibited characteristic absorption bands corresponding to O–H/N–H stretching (~3414 cm^{-1}), aliphatic C–H stretching (~3041 cm^{-1}), ester C=O stretching (~1690 cm^{-1}), and C–O stretching (~1228 cm^{-1}). DSPE-PEG$_{2000}$ displayed characteristic aliphatic C–H stretching vibrations (~3015 cm^{-1}) along with a prominent C–O–C stretching band at ~1060 cm^{-1}, confirming the presence of PEG moieties. Hyaluronic acid exhibited a broad O–H stretching band (~3216 cm^{-1}), characteristic carboxylate asymmetric and symmetric stretching bands at ~1606 and ~1397 cm^{-1}, respectively, and an amide I band at ~1658 cm^{-1}, consistent with its polysaccharide structure [31]. The FTIR spectrum of HA-LPs-F18 retained the characteristic peaks of rivastigmine tartrate, DSPE-PEG$_{2000}$, and hyaluronic acid, with only slight shifts in peak positions and reduced peak intensities. These spectral changes indicate successful encapsulation of rivastigmine tartrate and effective HA coating on the liposomal surface without the formation of new absorption bands or disappearance of characteristic functional groups, confirming the absence of significant chemical interactions or incompatibility among the formulation components.

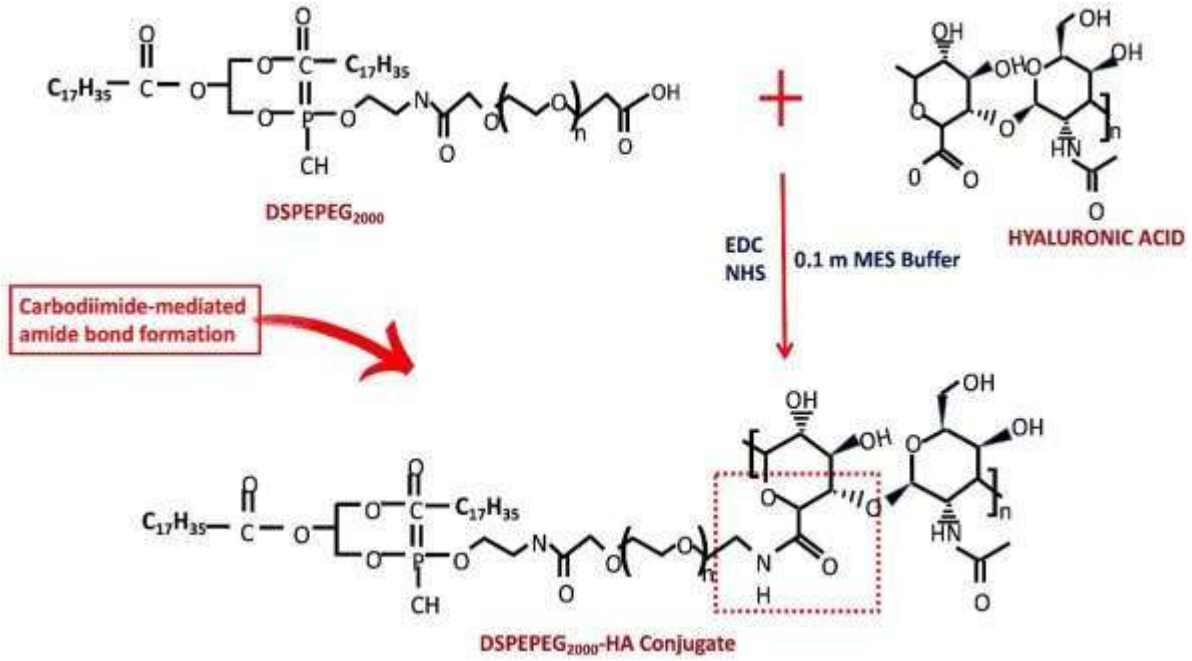

Figure 5. Formation of the HA–DSPE-PEG2000 conjugate via activation of HA and subsequent amide bond formation

3.4. *In-vitro* drug release study

The characteristic biphasic drug release profile of the HALPs-F18 was characterized by an initial burst release of 19.54% within the first 5 min, primarily attributed to the fraction of drug adsorbed on or associated with the liposomal surface. This rapid release was followed by a sustained, diffusion-controlled phase, during which the cumulative drug release gradually increased to 37.7% at 60 min and reached 57.54% after 350 min (**Figure 6**). The prolonged release pattern suggests efficient encapsulation of the drug within the liposomal core, while the hyaluronic acid (HA) coating acted as a diffusion barrier, modulating drug release and minimizing premature leakage. These findings demonstrate the capability of the HALP formulation to provide controlled and extended drug delivery, making it a promising system for prolonged therapeutic applications.

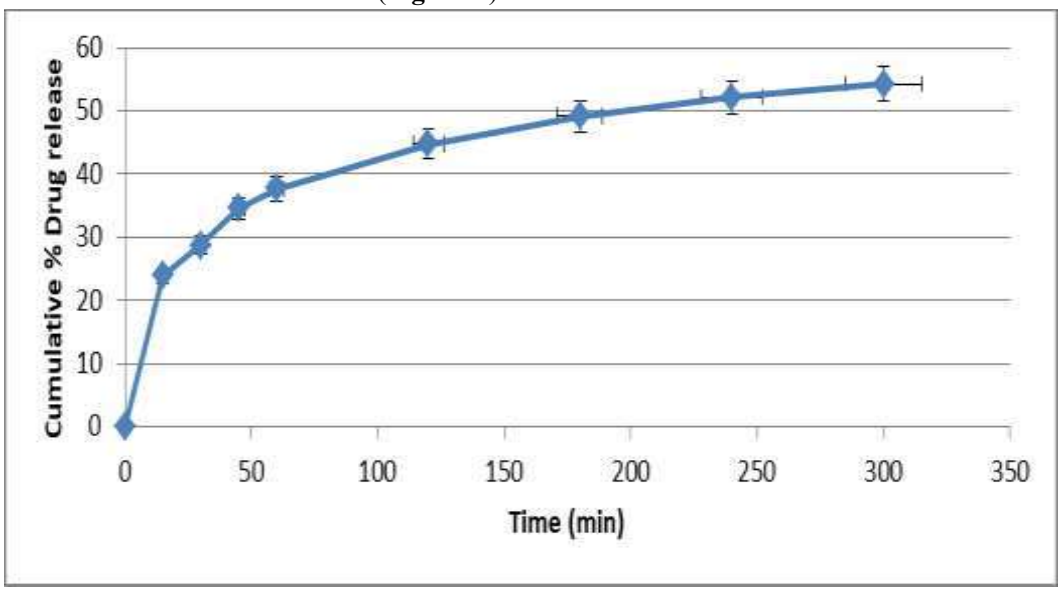

Figure 6: *In-vitro* drug release profile of HALPs-F18 formulation

3.5. Morphological analysis

3.5.1. Transmission electron microscopy (TEM)

TEM analysis (**Figure 7**) revealed that the prepared HALPs-F18 liposomes were predominantly spherical with a uniform size distribution. The vesicles exhibited smooth, well-defined bilayered structures and were free from noticeable aggregation, indicating excellent structural integrity and colloidal stability. The average particle size observed by TEM was approximately 100 nm, confirming the successful formation of nanosized liposomes suitable for targeted drug delivery applications.

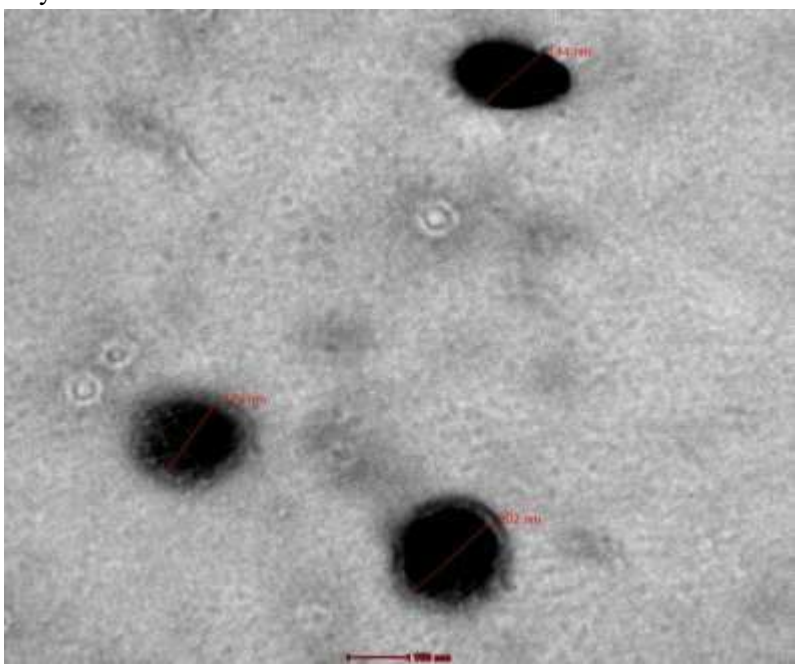

Figure 7: TEM microscopy of HALPs-F18

3.6. Stability study of HALPs-F18

The stability of the enhanced coated liposomal formulations was evaluated over a period of 90 days under two storage conditions: room temperature (25 ± 2°C) and refrigerated temperature (4 ± 2°C). A gradual increase in vesicle size was observed under both conditions throughout the storage period. However, the increase was minimal under refrigerated conditions, indicating satisfactory physical stability of the formulation. In contrast, liposomes stored at 25 ± 2°C exhibited a marked increase in vesicle size after 45 days, suggesting vesicle aggregation and reduced stability at elevated temperatures. The formulation also demonstrated effective retention of the encapsulated drug under refrigerated storage, as evidenced by only a slight reduction in entrapment efficiency [32]. Conversely, a significant decline in entrapment efficiency was observed at room temperature, indicating increased drug leakage during storage. Overall, as illustrated in **Figure 8**, the findings demonstrate that refrigerated storage effectively preserves vesicle integrity and drug entrapment efficiency, thereby enhancing the long-term stability of the coated liposomal formulation.

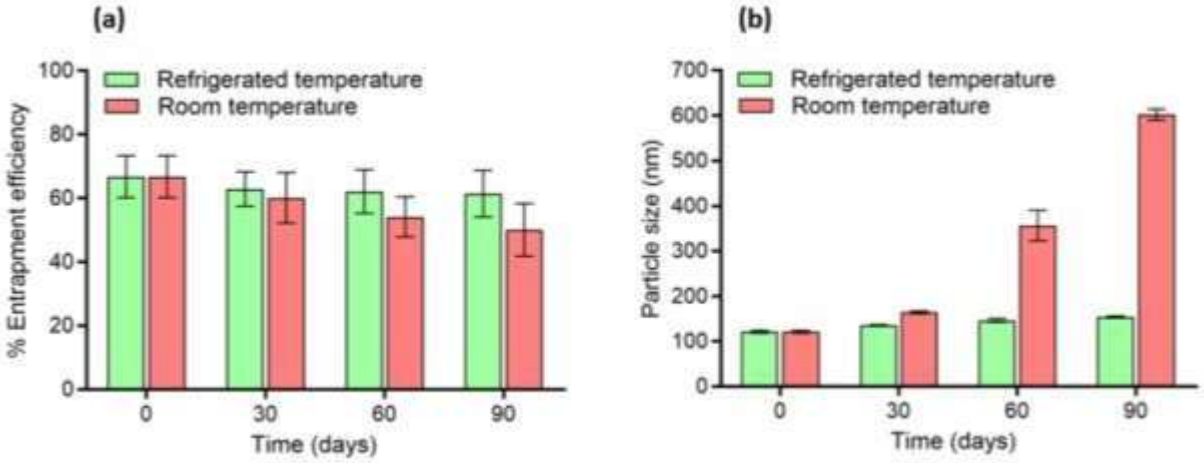

Figure 8. Stability assessment of HALPs-F18 at two storage temperatures: (a) Variation in entrapment efficiency at 4°C and 25°C; (b) Variation in particle size at 4°C and 25°C. Values are expressed as mean ± SD (n = 3).

3.7. *In-vivo* toxicity evaluation

3.7.1. Acute toxicity Study

An acute toxicity study was performed to evaluate the safety of the intranasal rivastigmine tartrate -loaded liposomal formulation (HALPs-F18) in Wistar rats at a dose of 0.5 mg/kg. Animals were allocated into control (PBS), plain liposome, and HALPs-F18 treatment groups, including both male and female rats (n = 3-6 per group). Throughout the 14-day observation period, no mortality, signs of toxicity, or abnormal behavioral changes were observed in any of the experimental groups. Furthermore, no statistically significant differences were detected in hematological indices, biochemical parameters, body weight, or relative organ weights between the treated and control groups (one-way ANOVA, $p > 0.05$). These findings indicate that intranasal administration of HALPs-F18 is well tolerated and does not produce any observable acute toxic effects under the conditions of this study.

3.7.2. Hematological Parameters

Hematological analysis demonstrated comparable values among the control (PBS), plain liposome, and HALPs-F18-treated groups in both male and female Wistar rats. Hemoglobin concentrations ranged from 12.96 to 16.40 g/dL, platelet counts from 9.16 to 13.03 × 10^5/mm³, and red blood cell (RBC) counts from 4.00 to 5.73 × 10^6/mm³. Similarly, packed cell volume (PCV; 34.5–46.6%), mean corpuscular volume (MCV; 79.6–91.0 fL), mean corpuscular hemoglobin (MCH; 20.4–24.7 pg), and total leukocyte count (TLC; 4.8–6.3 × 10^9/L) showed no significant treatment-related variations. Differential leukocyte counts, including neutrophils (27.7–43.6%) and lymphocytes (61.9–71.8%), were also comparable among the experimental groups (**Table 3**). Statistical analysis revealed no significant differences in any hematological parameter between the treatment and control groups (one-way ANOVA, $p > 0.05$). All measured values remained within normal physiological ranges, indicating that intranasal administration of the HALPs-F18 formulation did not induce any adverse hematological effects at the tested dose.

Table 3: Hematological parameters in intranasal acute toxicity study

Treatment Group	Control	Plain liposome	HALPs-F18 (0.5 mg/kg)	Control	Plain liposome	HLPs-F18 (0.5 mg/kg)
	Male			Female		
Haemoglobin (gm/dl)	15.73±1.47	16.4±1.7	15.13±1.15	13.73±1.33	13.76±1.45	12.96±1.47
Platelet Count (lacs/mm^3)	10.33±1.02	13.03±1.97	10.16±1.30	11.8±1.35	11.2±1.00	9.16±0.90
RBC (10^6/mm^3)	4.00±0.75	4.33±1.36	4.2±2.38	4.8±0.52	5.73±1.01	5.1±0.88
PCV (%)	37.06±6.07	36.7±4.5	34.5±6.1	46.6±5.2	43.2±5.7	39.3±6.05

*Author for Correspondence: jainmansha1@gmail.com

MCV (fL)	91.0±4.09	87.3±3.5	87.2±9.7	82.83±3.8	79.6±8.6	87.2±4.2
MCH (pg)	21.6±5.1	24.6±4.5	22.8±4.4	21.6±6.1	20.4±2.5	24.7±4.6
TLC (10^9/L)	6.3±0.8	5.7±0.4	5.4±1.1	5±0.75	5.7±1.1	4.8±1.7
Differential leukocyte count						
Neutrophil	43.6±4.2	40.1±3.6	35.4±2.9	33.7±4.5	33.4±6.0	27.7±2.5
Lymphocyte	61.2±4.4	64±7.9	68.7±8.9	71.8±6.2	65.2±10.1	61.9±12.7
Eosinophil	1.0±0.15	1.1±0.2	1.2±0.4	1.2±0.3	0.97±0.1	0.8±0.2
Monocyte	1.3±0.4	1.1±0.35	0.9±0.2	2.0±0.3	1.9±0.3	1.6±0.1
Basophil	0.29±0.16	0.26±0.16	0.21±0.10	0.10±0.09	0.22±0.05	0.21±0.03

Values are expressed as mean ± SD (n = 3 per group). One-way ANOVA followed by Dunnet's test. RBC= Red Blood Cell count, PCV= Packed Cell Volume, MCV=Mean Corpuscular Volume, MCH=Mean Corpuscular Hemoglobin.

3.7.3. Serum Biochemical Analysis

Serum biochemical analysis demonstrated no significant differences between the control (PBS), plain liposome, and HALPs-F18-treated groups in either male or female Wistar rats. Renal function markers, including blood urea nitrogen (BUN; 35.6–44.2 mg/dL) and serum creatinine (0.30–0.33 mg/dL), remained within normal physiological ranges. Likewise, liver function parameters, including alkaline phosphatase (ALP; 42.3–50.1 U/L), aspartate aminotransferase (AST; 121.9–148.8 U/L), and alanine aminotransferase (ALT; 31.6–36.0 U/L), showed no treatment-related alterations. Lipid profile parameters, including total cholesterol (71.8–79.7 mg/dL) and triglycerides (39.6–48.6 mg/dL), were comparable across all experimental groups. In addition, serum electrolytes, albumin (4.6–5.3 g/dL), glucose (108.9–128.1 mg/dL), and total protein (5.1–5.8 g/dL) remained unchanged following treatment. Statistical analysis revealed no significant differences in any biochemical parameter between the treated and control groups (one-way ANOVA, $p > 0.05$). These findings indicate that intranasal administration of the rivastigmine tartrate -loaded liposomal formulation (HALPs-F18) did not induce hepatotoxicity, nephrotoxicity, or metabolic disturbances at the tested dose (**Table 4**).

Table 4: Serum biochemical analysis in intranasal acute toxicity study

Treatment Group	**Control**	**Plain liposome**	**Rivastigmine tartrate liposomes (0.5 mg/kg)**	**Control**	**Plain liposome**	**Rivastigmine tartrate liposomes (0.5 mg/kg)**
	Male			**Female**		
ALP (U/I)	46.3±5.6	49.3±6.4	42.3±5.4	45.2±6.5	50.1±7.6	42.4±4.3
AST (U/L)	123.2±8.75	122.5±11.9	148.8±26.3	123.06±20.36	133.6±6.7	121.9±9.9
ALT (U/I)	35.7±7.47	33.4±5.5	35.6±8.5	36.0±5.6	31.6±4.6	33.9±4.1
Bilirubin Total (mg/dl)	0.20±0.03	0.15±0.03	0.20±0.04	0.15±0.03	0.13±0.04	0.14±0.04
Bilirubin Direct (mg/dl)	0.033±0.05	0.033±0.05	0.033±0.05	0.036±0.05	0.02±0.01	0.02±0.01

BUN (mg/dl)	39.7±6.7	37.2±3.7	39.6±2.3	44.2±3.9	35.9±5.1	35.6±4.8
Uric acid (mg/dl)	1.2±0.28	1.5±0.25	1.4±0.26	1.3±0.3	1.3±0.3	1.5±0.2
Creatinine (mg/dl)	0.32±0.05	0.30±0.08	0.30±0.02	0.31±0.05	0.32±0.04	0.33±0.04
Total Protein (g/dl)	5.8±1.0	5.8±0.7	5.2±0.75	5.1±0.6	5.2±0.5	5.7±1.1
Albumin (g/dl)	5.3±1.0	4.6±0.5	4.7±0.31	5.1±0.15	4.8±0.95	4.8±0.65
Calcium (mg/dl)	10.3±1.05	10.7±0.6	9.9±0.6	10.6±0.6	9.1±1.0	10.2±0.8
Glucose (mg/dl)	116.5±9.3	128.1±4.6	123.9±5.0	114.6±8.5	108.9±8.0	116.3±4.5
Total Cholesterol (mg/dl)	71.8±9.5	74.4±13.3	73.3±3.8	79.7±6.5	75.3±5.02	79.3±5.70
Triglyceride (mg/dl)	39.6±6.39	48.6±2.01	46.0±7.7	43.9±3.6	42.9±3.1	44.2±4.1
HDL-C (mg/dl)	76.03±5.9	77.5±2.9	79.2±8.8	79.7±6.5	75.3±5.0	79.3±5.7
VLDL (mg/dl)	6.7±0.41	6.0±0.5	6.1±0.2	6.7±0.41	7.2±0.6	7.0±0.5

Values are expressed as mean ± SD (n = 6 per group). One-way ANOVA followed by Tukey's post-hoc test. ALP= alkaline phosphatase, AST= aspartate aminotransferase, ALT=alanine aminotransferase, BUN= blood urea nitrogen, HDL=High Density Lipoprotein, VLDL= Very-Low-Density Lipoprotein.

4. Discussion

Intranasal administration has emerged as a promising non-invasive strategy for direct brain targeting because it enables therapeutic agents to bypass the blood–brain barrier (BBB) through the olfactory and trigeminal neuronal pathways. Despite this advantage, rapid mucociliary clearance and limited epithelial permeability remain major challenges that reduce drug residence time, absorption, and overall therapeutic efficacy. Liposomal formulations offer an effective approach to overcome these limitations owing to their excellent biocompatibility, ability to enhance drug solubility, and capacity to protect encapsulated drugs from enzymatic degradation within the nasal cavity [33]. Furthermore, surface functionalization of liposomes with HA enhances mucoadhesion, thereby prolonging nasal residence time and facilitating sustained drug absorption. HA can also promote receptor-mediated uptake through interactions with CD44 receptors expressed on nasal epithelial cells. Previous studies have demonstrated that HA-coated lipid nanocarriers improve mucosal adhesion, physicochemical stability, and brain-targeting efficiency following intranasal administration. Moreover, nanosized liposomes with an appropriate surface charge and high drug-loading capacity are considered highly suitable for enhanced nose-to-brain transport and sustained drug release [34].

In the present study, HA-coated rivastigmine tartrate - loaded liposomes (HALPs-F18) were successfully developed and optimized as a potential intranasal delivery system. The optimized formulation exhibited a

mean vesicle size of 121.36 ± 3.05 nm with a low polydispersity index, indicating a homogeneous nanosized population that is favorable for efficient nasal uptake and transport to the brain. The DLS analysis yielded a representative Z-average diameter of 118.3 nm in an individual measurement, whereas the reported vesicle size represents the mean of three independent measurements, confirming excellent reproducibility. TEM study showed vesicle diameters ranging from 144 to 202 nm, which were larger than those obtained by DLS. This difference is expected because DLS measures the hydrodynamic diameter of hydrated vesicles in suspension, whereas TEM determines the physical diameter of dehydrated particles. In addition, dehydration and minor vesicle aggregation during TEM sample preparation may contribute to the apparent increase in particle size observed in the micrographs.

The optimized formulation achieved a high entrapment efficiency of 65.78 ± 6.6%, indicating efficient incorporation of rivastigmine tartrate within the lipid bilayer and suggesting the potential for sustained drug release [30]. Following HA coating, the zeta potential shifted toward more negative values, confirming successful surface functionalization and indicating enhanced colloidal stability through increased electrostatic repulsion between vesicles. FTIR spectroscopy further demonstrated the successful incorporation of formulation components. The characteristic absorption bands of rivastigmine tartrate, DSPE-PEG2000, and HA were retained with only minor shifts in peak position and intensity, indicating the absence of chemical incompatibility or degradation during formulation. Collectively, these physicochemical findings confirm the successful preparation of a stable HA-coated liposomal system with characteristics favorable for intranasal brain-targeted delivery of rivastigmine tartrate.

5. Conclusion

In the present study, hyaluronic acid-coated liposomes were successfully developed and optimized as a nanoscale intranasal delivery system for rivastigmine tartrate. The optimized HALPs exhibited favorable physicochemical properties, including an appropriate vesicle size, high drug entrapment efficiency, sustained drug release, and satisfactory stability, demonstrating the structural integrity and robustness of the formulation. Statistical optimization further validated the reliability and predictive capability of the experimental design. Moreover, intranasal administration of HALPs to Wistar rats did not produce any significant alterations in hematological, biochemical, or physiological parameters, indicating good biocompatibility and safety following acute treatment. Overall, these findings suggest that HALPs represent a promising and biocompatible nanocarrier platform for efficient nose-to-brain delivery of rivastigmine tartrate. This delivery strategy has the potential to enhance brain targeting, improve therapeutic efficacy, and reduce systemic side effects, making it a promising approach for the management of Alzheimer's disease. Further long-term preclinical and clinical investigations are warranted to establish its therapeutic potential and translational applicability.

Conflict of interest

The authors declare that they have no conflicts of interest, financial or otherwise, in relation to this work.

Funding

No funding was received for this study

Clinical trial number

Not applicable

Acknowledgements

The authors gratefully acknowledge the Adina Institute of Pharmaceutical Sciences, Sagar, for their support and facilities provided during this research..

REFERENCES

1. Vohra M, Amir M, Sharma A, Wadhwa S. Formulation strategies for nose-to-brain drug delivery in Alzheimer's disease. Health Sci Rev. 2023; 6:100075.
2. Zolkiffly SZI, Hasan MH, Jusoh SA, Janakiraman AK, Eshak Z, Sukumaran SK, et al. Investigating the effects of nanoformulated fisetin in Alzheimer's disease: From molecular docking to pharmacotherapeutic potential. Eur J Pharmacol. 2025;177967.
3. Iqubal A, Iqubal MK, Fazal SA, Pottoo FH, Haque SE. Nutraceuticals and their derived nano-formulations for the prevention and treatment of Alzheimer's disease. Curr Mol Pharmacol. 2022;15(1):23–50.
4. Lv H, Wang Y, Yang X, Ling G, Zhang P. Application of curcumin nanoformulations in Alzheimer's disease: Prevention, diagnosis and treatment. Nutr Neurosci. 2023;26(8):727–742.
5. Gao Y, Almalki WH, Afzal O, Panda SK, Kazmi I, Alrobaian M, et al. Systematic development of lectin-

conjugated microspheres for nose-to-brain delivery of rivastigmine for the treatment of Alzheimer's disease. Biomed Pharmacother. 2021; 141:111829.
6. Salade L, Wauthoz N, Vermeersch M, Amighi K, Goole J. Chitosan-coated liposome dry-powder formulations loaded with ghrelin for nose-to-brain delivery. Eur J Pharm Biopharm. 2018; 129:257–266.
7. Shah BM, Misra M, Shishoo CJ, Padh H. Nose-to-brain microemulsion-based drug delivery system of rivastigmine: Formulation and ex vivo characterization. Drug Deliv. 2015;22(7):918–930.
8. Nageeb El-Helaly S, Abd Elbary A, Kassem MA, El-Nabarawi MA. Electrosteric stealth rivastigmine-loaded liposomes for brain targeting: Preparation, characterization, ex vivo biodistribution and in vivo pharmacokinetic studies. Drug Deliv. 2017; 24(1):692–700.
9. Guo H, Wang G, Zhai Z, Huang J, Huang Z, Zhou Y, et al. Rivastigmine nasal spray for the treatment of Alzheimer's disease: Olfactory deposition and brain delivery. Int J Pharm. 2024; 652:123809.
10. Lee D, Shen AM, Garbuzenko OB, Minko T. Liposomal formulations of anti-Alzheimer drugs and siRNA for nose-to-brain delivery: Design, safety and efficacy in vitro. AAPS J. 2024; 26(5):99.
11. Horvát S, Fehér A, Wolburg H, Sipos P, Veszelka S, Tóth A, et al. Sodium hyaluronate as a mucoadhesive component in nasal formulations enhances delivery of molecules to brain tissue. Eur J Pharm Biopharm. 2009; 72(1):252–259.
12. Serri C, Quagliariello V, Cruz-Maya I, Guarino V, Maurea N, Giunchedi P, et al. Hyaluronic acid-based nanoparticles loaded with rutin as vasculoprotective tools against anthracycline-induced endothelial damage. Pharmaceutics. 2024;16(8):985.
13. Serri C, Piccioni M, Guarino V, Santonicola P, Cruz-Maya I, Crispi S, et al. Hyaluronic acid-based hybrid nanoparticles as promising carriers for the intranasal administration of dimethyl fumarate. Int J Nanomedicine. 2025; 20:71–89.
14. AbouElhassan KM, Sarhan HA, Hussein AK, Taye A, Ahmed YM, Safwat MA. Brain targeting of citicoline sodium via hyaluronic acid-decorated novel nano-transbilosomes for mitigation of Alzheimer's disease in a rat model: Formulation, optimization, in vitro and in vivo assessment. Int J Nanomedicine. 2022; 17:6347–6368.
15. Narayan R, Singh M, Ranjan O, Nayak Y, Garg S, Shavi GV, et al. Development of risperidone liposomes for brain targeting through the intranasal route. Life Sci. 2016; 163:38–45.
16. Hebbar S, Poonja M, Shetty A, Dubey A. In vitro investigation of conventional, chitosan-coated and electrosteric stealth liposomes of rivastigmine for the treatment of Alzheimer's disease. Int J Pharm Investig. 2020;10(4).
17. Shnaikat SG, Shakya AK, Bardaweel SK. Formulation, development and evaluation of hyaluronic acid-conjugated liposomal nanoparticles loaded with regorafenib and curcumin and their in vitro evaluation on colorectal cancer cell lines. Saudi Pharm J. 2024;32(7):102099.
18. Khairnar P, Singh A, Ahirwar K, Shukla R. ApoE3-anchored liposomal delivery of rivastigmine for brain delivery: Formulation, characterization and in vivo pharmacokinetic evaluation. AAPS PharmSciTech. 2023; 24(8):223.
19. Ravar F, Saadat E, Gholami M, Dehghankelishadi P, Mahdavi M, Azami S, et al. Hyaluronic acid-coated liposomes for targeted delivery of paclitaxel: In vitro characterization and in vivo evaluation. J Control Release. 2016; 229:10–22.
20. Zhang P, Tang J, Cheng L, Xue Y, Yang J, Sun Z, et al. Hyaluronic acid-modified liposomes with enhanced transdermal delivery of methotrexate for psoriasis treatment. Colloids Surf B Biointerfaces. 2025; 247:114457.
21. Huang J, Chen J. Pharmacokinetics and pharmacodynamic evaluation of hyaluronic acid-modified imatinib-loaded PEGylated liposomes in CD44-positive GIST882 tumor-bearing mice. J Liposome Res. 2024; 34(1):97–112.
22. Lombardo D, Kiselev MA. Methods of liposome preparation: Formation and control factors of versatile nanocarriers for biomedical and nanomedicine applications. Pharmaceutics. 2022; 14(3):543.
23. Alexandar S, Diwedi R, Ashok T, Chandrasekhar MJN. A validated RP-HPLC method for estimation of rivastigmine in pharmaceutical formulations. Der Pharm Lett. 2011; 3(3):421–426.
24. Ravi G, Guptas NV. Development and evaluation of transdermal films containing solid lipid nanoparticles of rivastigmine. Int J Appl Pharm. 2017; 9:85–90.
25. Sun Y, Shen X, Yang J, Tan C. Hyaluronic acid-coated nanoliposomes as delivery systems for fisetin: Stability, membrane fluidity and bioavailability. Foods. 2024;13(15):2406.
26. Harthi S, Alavi SE, Radwan MA, El Khatib MM, AlSarra IA. Nasal delivery of donepezil HCl-

loaded hydrogels for the treatment of Alzheimer's disease. Sci Rep. 2019; 9(1):9563.
27. Thakurdesai P, Deshpande P. Preclinical safety evaluation of acute and subacute intranasal administration of polyphenol-based cinnamon bark extract in laboratory rats. Pharmacogn J. 2021; 13(6 Suppl).
28. Emami A, Tepper J, Short B, Yaksh TL, Bendele AM, Ramani T, et al. Toxicology evaluation of drugs administered via uncommon routes: Intranasal, intraocular, intrathecal/intraspinal and intra-articular. Int J Toxicol. 2018; 37(1):4–27.
29. Rao BLN, Krishnan SP, Reddy CB. Application of Box–Behnken design and desirability function in the development and optimization of stealth liposomes of a microtubule inhibitor. J Pharm Res Int. 2021; 33(47A):563–575.
30. Sabir F, Katona G, Pallagi E, Dobó DG, Akel H, Berkesi D, et al. Quality-by-design-based development of n-propyl gallate-loaded hyaluronic acid-coated liposomes for intranasal administration. Molecules. 2021; 26(5):1429.
31. Pattni BS, Chupin VV, Torchilin VP. New developments in liposomal drug delivery. Chem Rev. 2015; 115(19):10938–10966.
32. Akbarzadeh A, Rezaei-Sadabady R, Davaran S, Joo SW, Zarghami N, Hanifehpour Y, et al. Liposome: Classification, preparation and applications. Nanoscale Res Lett. 2013; 8(1):102.
33. Djupesland PG. Nasal drug delivery devices: Characteristics and performance in a clinical perspective—a review. Drug Deliv Transl Res. 2013; 3(1):42–62.
34. Huang G, Huang H. Application of hyaluronic acid as carriers in drug delivery. Drug Deliv. 2018; 25(1):766–772..